

# Investigating Arylazoformamide Ligands in Palladium(II) Precatalysts through the Suzuki–Miyaura Cross-Coupling Reaction

Laxmi Tiwari, Elliott B. Hulley,\* and Kristopher V. Waynant\*



Cite This: *J. Org. Chem.* 2024, 89, 17917–17925



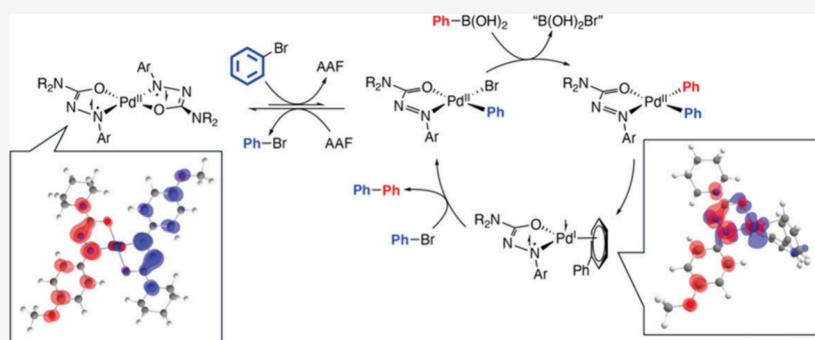
Read Online

ACCESS |

Metrics & More

Article Recommendations

Supporting Information



**ABSTRACT:** Herein, is the reported synthesis and utilization of redox-active arylazoformamide (AAF) ligands in palladium(II) precatalysts for the Suzuki–Miyaura cross-coupling reaction. Complexes were formed from 2 equiv of an AAF ligand with  $\text{Pd}(\text{II})\text{Cl}_2$  in an appropriate solvent to create the square planar  $(\text{AAF})_2\text{PdCl}_2$  precatalyst. A thorough investigation of aryl bromides and arylboronic acids found that 1.0 mol % precatalyst with cesium carbonate ( $\text{Cs}_2\text{CO}_3$ ) as base, 1,4-dioxane as solvent at  $90^\circ\text{C}$  for 24 h allowed for excellent conversions to the biphenyl products (over 20 examples). To highlight the AAF ligand class, a set of comparison reactions were performed with redox-active arylazothioformamide ligands, i.e., an  $(\text{ATF})_2\text{PdCl}_2$  complex, other commercial palladium(II) complexes, and a  $\text{Ni}(\text{II})\text{Cl}_2$  arylazoformamide coordination complex. The  $(\text{AAF})_2\text{PdCl}_2$  complexes outperformed all of others tested. Mechanistically, it is proposed that the AAF ligand singly reduces to antiferromagnetically couple to the palladium(I) complex as a transmetalation intermediate. Ni-based precatalysts were found to be inactive for the studied Suzuki–Miyaura reaction. Overall, these ligand systems offer a unique look into redox-active palladium cross-coupling reactions as well as being phosphine-free and high yielding.

## INTRODUCTION

The palladium catalyzed Suzuki–Miyaura coupling reaction has become one of the most effective and efficient methods for the synthesis of complex organic molecules and diverse bioactive compounds.<sup>1–3</sup> The reaction holds a pivotal position for forming carbon–carbon (C–C) bonds, using readily available aryl halides and arylboronic acids and has been a well-utilized resource for multiple applications.<sup>4–6</sup> In a homogeneous reaction environment, phosphine ligands assume a crucial role in facilitating C–C bond formation under conditions characterized by an inert atmosphere and the absence of moisture.<sup>7,8</sup> Due to the air- and moisture-sensitive nature of many phosphine ligands, there is a susceptibility for P–C bond degradation under elevated temperatures. This phenomenon can result in the contamination of the associated metal, consequently inducing catalyst decomposition and significantly impacting both conversion and selectivity in catalytic processes.<sup>9–11</sup> So, the pursuit of phosphine-free ligand catalysts has emerged as a critically important focus within the field. Various alternatives to phosphines, such as amines, N-heterocyclic carbenes, oximes, and hydrazones, have been

explored.<sup>11–13</sup> Semicarbazones have been promising as ligands for Suzuki–Miyaura reactions due to their advantages in shelf life, selectivity, and environmental compatibility.<sup>14</sup> Arylazoformamides (AAF) and Arylazothioformamides (ATF), a subclass of semicarbazone and thiosemicarbazone ligands with  $\text{N}^+\text{O}/\text{S}$ -donor capabilities, have garnered attention due to their versatile coordination and biological potential.<sup>15–18</sup> Catalytic carbon–carbon coupling reactions are mediated by complexes bearing ligands that support a variety of coordination modes, metal preference, and the ability to form ligand-localized redox states. The incorporation of sterically hindered ligands in Suzuki–Miyaura coupling reactions proves advantageous as these ligands can effectively promote the oxidative addition

Received: April 30, 2024

Revised: August 18, 2024

Accepted: October 31, 2024

Published: December 4, 2024



**Scheme 1. Synthesis of AAF Ligand and Resulting Pd and Ni Complexes, 3a, 3b, and 5; Synthesis of ATF Ligand and  $\text{PdCl}_2(\text{ATF})_2$  Complex, 4**

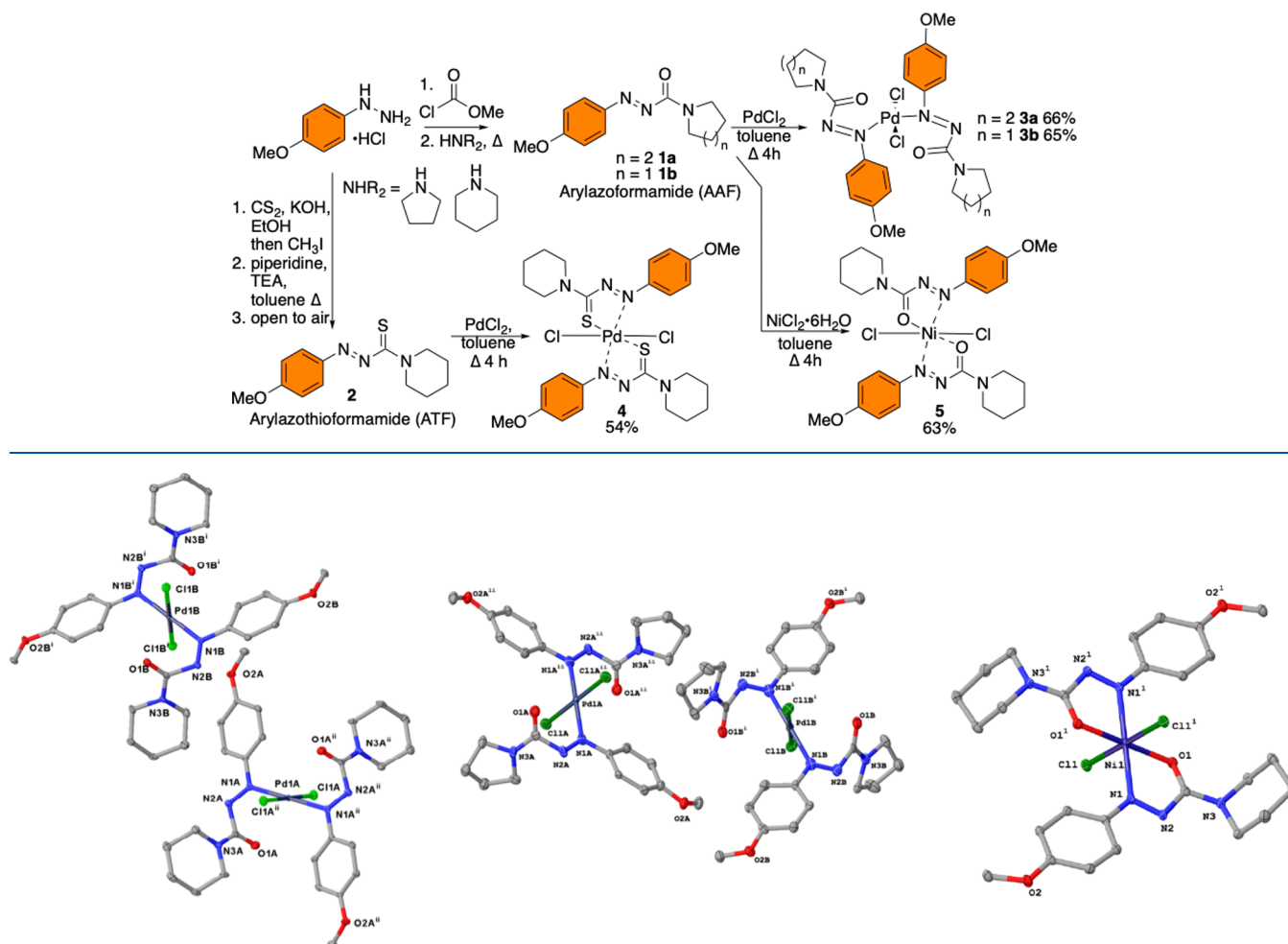


**Figure 1.** Crystal structures of complex 3a, 3b and 5. All thermal ellipsoids are drawn at the 50% probability level. Hydrogen atoms have been removed for the sake of clarity. Structures 3a and 3b both crystallize into two similar but unique structures ( $Z = 2$ ). Palladium complexes 3a and 3b are square planar while nickel complex 5 is octahedral.

and reductive elimination processes.<sup>19</sup> This enhancement facilitates the accommodation of a diverse array of substrates, thereby contributing to the versatility and efficiency of the catalytic reaction.<sup>20–22</sup>

In the context of this study, AAF and ATF ligands were investigated as ligands in palladium(II) precatalysts to evaluate their utility in Suzuki–Miyaura coupling reactions. AAF ligands with piperidine- or pyrrolidine-based formamide components emerged as strong contenders for Suzuki coupling reactions. Others have shown that the deliberate introduction of diverse functional groups into the ligand environment enables precise control over both steric and electronic characteristics of the ligands.<sup>23–25</sup> AAF/ATF ligands incorporating steric and electron-donating (*p*-MeO) groups have been shown to enhance binding association equilibria as well as catalytic performance in  $\text{CO}_2$  insertion reactions.<sup>26,27</sup> DFT calculations (*vide infra*) have shown that both AAF and ATF ligands are redox noninnocent, and the stabilization of reduced redox states plays a significant role in their behavior in catalysis.<sup>28</sup> Herein, the synthesis of Suzuki-type coupling precatalyst complexes is presented, utilizing AAF and ATF

ligands, and the limitations, scope, optimization, and catalytic activity with various substrates.

## RESULTS AND DISCUSSION

Ligands 1a, 1b, and 2 were synthesized according to previously published literature and shown in Scheme 1.<sup>15,17</sup> Palladium(II) and nickel(II) complexes (3a, 3b, and 5) formed in good yield from palladium(II) chloride or nickel(II) chloride hexahydrate in toluene, respectively. These new complexes were found to be air and moisture stable and were confirmed by  $^1\text{H}$  and  $^{13}\text{C}$  NMR, FTIR, and elemental analysis along with single crystal X-ray diffraction (see Supporting Information, SI). The reaction pathway for the synthesis of the piperidine substituted *p*-methoxyphenylazothioformamide palladium(II) complex (4) resulted from refluxing ATF (2) with palladium(II) chloride in toluene is also shown in Scheme 1. Complex 4 appears to be two ATFs with a  $\text{Pd}(\text{II})\text{Cl}_2$  salt. NMR shifts, elemental analysis, and previous results suggest that coordination is through both the nitrogen and sulfur atoms.

The crystal structures of complexes 3a, 3b and 5 are shown in Figure 1, and crystallographic data can be found in the SI (Tables S1–S4) with selected bond lengths and bond angles

**Table 1. Optimization Studies for Pd-Catalyzed Suzuki–Miyaura Sequence of Bromobenzene with Phenylboronic Acid<sup>a</sup>**

Entry	Solvent	Base	Precatalyst loading (Mol%)	Temp	Time (h)	Yield <sup>b</sup> (%)	TON <sup>c</sup>	TOF (h <sup>-1</sup> ) <sup>d</sup>
1	DMSO	Cs <sub>2</sub> CO <sub>3</sub>	1	90 °C	20	75	75	3.75
2	DMF	Cs <sub>2</sub> CO <sub>3</sub>	1	90 °C	20	90	90	4.5
3	Toluene	Cs <sub>2</sub> CO <sub>3</sub>	1	90 °C	20	86	86	4.3
4	1,4-Dioxane	Cs <sub>2</sub> CO <sub>3</sub>	1	90 °C	20	94	94	4.7
5	THF	Cs <sub>2</sub> CO <sub>3</sub>	1	90 °C	20	10	10	0.5
6	1,4-Dioxane	K <sub>3</sub> PO <sub>4</sub>	1	90 °C	20	34	34	1.7
7	1,4-Dioxane	K <sub>2</sub> CO <sub>3</sub>	1	90 °C	20	39	39	1.95
8	1,4-Dioxane	Na <sub>2</sub> CO <sub>3</sub>	1	90 °C	20	8	8	0.4
9	1,4-Dioxane	Li(OH)·H <sub>2</sub> O	1	90 °C	20	18	18	0.9
10	1,4-Dioxane	Cs <sub>2</sub> CO <sub>3</sub>	1	RT	20	70	70	3.5
11	1,4-Dioxane	Cs <sub>2</sub> CO <sub>3</sub>	0.5	90 °C	20	90	90	9.09
12	1,4-Dioxane	Cs <sub>2</sub> CO <sub>3</sub>	0.1	90 °C	20	36	36	17.9
13	1,4-Dioxane	Cs <sub>2</sub> CO <sub>3</sub>	0.05	90 °C	20	21	21	20.8
14	1,4-Dioxane	Cs <sub>2</sub> CO <sub>3</sub>	1	90 °C	10	84	84	8.4
15	1,4-Dioxane	Cs <sub>2</sub> CO <sub>3</sub>	1	90 °C	5	71	71	14.2

<sup>a</sup>Reaction conditions: bromobenzene (1.0 mmol), phenylboronic acid (1.2 mmol), base (2 mmol), solvent (4 mL) under inert conditions.

<sup>b</sup>Isolated yield, <sup>c</sup>Mole product/mol catalyst, <sup>d</sup>TON/time.

listed in Table S5. Notably, all complexes crystallized in triclinic geometry with the P1 space group. Pd centers in (3a) and (3b) complexes display square planar geometry whereas the Ni center in (5) shows distorted octahedral geometry with O–Ni–N angles of 76.03° inside the chelate and 103.97° outside the chelate. To note, AAF ligands in palladium(II)-chloride precatalyst complexes do not coordinate through the oxygen atom, and the AAF torsional angles of 62.13° and 64.69° indicate that the N=N–C=O motif is not aligned through the *p*-orbital system. Moreover, the Pd–O distances are 3.018 and 3.049 Å while the Pd–N distances are 2.025 and 2.029 Å resulting in a square planar coordination geometry with the chloride ions. Yet, the Ni(II) AAF complex does coordinate through the oxygen atoms of the AAF and gives Ni–O distances of 2.037 Å to complement the Ni–N distances of 2.095 Å in addition to the aligned *p*-orbital system of the N=N–C=O torsional angle of 9.78°.

With the new complexes in hand, a comprehensive examination was performed to determine the most favorable parameters for Suzuki–Miyaura cross-coupling. Utilizing bromobenzene and phenylboronic acid as the substrates for the initial screening, and starting with solvent choice, DMSO, DMF, toluene, 1,4-dioxane, and THF were tested using Cs<sub>2</sub>CO<sub>3</sub> as the base and under increased temperatures as reported by others.<sup>29–31</sup> Shown in Table 1, entry 4, 1,4-dioxane was the most effective solvent yielding the biphenyl product in 94% yield, where THF exhibited a significantly lower yield at just 10% (Table 1, entry 5). Experiments were conducted at both room temperature and 90 °C, and it was evident that higher temperatures favored greater product yield (Table 1, entry 10). Notably, 90 °C, while under the reflux temperature of the remaining solvents (DMSO, DMF, toluene), was chosen as 1,4-dioxane performed best at this temperature. Moving on, various inorganic bases were tested (Table 1, entries 5–9) with Cs<sub>2</sub>CO<sub>3</sub> outperforming all inorganic bases tested. As expected, higher catalyst loadings led to increased product formation, whereas lower catalyst percentages diminished yields over the 20 h period (Table 1,

entries 4, 11, 12, and 13). Ultimately, at 1 mol % precatalyst loading with an agreeable 24 h reaction time, a variety of results ranging from 71% to 94%, categorized as good to excellent, were found (Table 1, entries 4, 14, and 15).

To verify that complex (3a) is the ideal catalyst for the phosphine-free Suzuki–Miyaura cross-coupling reaction, other catalysts were evaluated under optimized conditions. The results of the catalytic activities for complexes (3a), (3b), (4), and (5), PdCl<sub>2</sub>, and Pd(PPh<sub>3</sub>)<sub>2</sub> salts are presented in Table 2. Complex (3a), denoted as PdCl<sub>2</sub>-piperidine-*p*-MeOAAF,

**Table 2. Catalytic Activities of Complexes and Pd Salts in Suzuki–Miyaura C–C Coupling Reaction under Optimized Conditions<sup>a</sup>**

Entry	Precatalyst	Yield <sup>a</sup> (%)
1	3a PdCl <sub>2</sub> (piperidine- <i>p</i> -MeOAAF) <sub>2</sub>	94
2	3b PdCl <sub>2</sub> (pyrrolidine- <i>p</i> -MeOAAF) <sub>2</sub>	84
3	4 PdCl <sub>2</sub> (piperidine- <i>p</i> -MeOATF) <sub>2</sub>	36
4	PdCl <sub>2</sub>	18
5	PdCl <sub>2</sub> (PPh <sub>3</sub> ) <sub>2</sub>	82
6	5 NiCl <sub>2</sub> (piperidine- <i>p</i> -MeOAAF) <sub>2</sub>	NR
7	No catalyst	NR

<sup>a</sup>Reaction conditions: bromobenzene (1.0 mmol), phenyl boronic acid (1.2 mmol), Cs<sub>2</sub>CO<sub>3</sub> (2 mmol), 1,4-dioxane (4 mL), catalyst (1 mol %) 20 h at 90 °C under inert atmosphere. <sup>b</sup>Isolated yield, NR = No Reaction.

provided the highest yield at 94%. Comparably, complex (3b) (PdCl<sub>2</sub>-pyrrolidine-*p*-MeOAAF) gave a slightly lower yield. A recent study on copper(I) salts with ATF ligands showed that pyrrolidine-ATFs have around three times higher binding association constants than piperidine-ATFs, demonstrating a metal to pyrrolidine-ATF interaction is stronger and more difficult to break.<sup>32</sup> In contrast, complex (4), PdCl<sub>2</sub>-piperidine-

*p*-MeOATF, produced biphenyl in a much lower yield (36%), again, potentially owing to the stronger coordination complex of the *thio* formamide. This result while low, contrasted the nonreactivity reported earlier with diethyl-ATF Pd complexes.<sup>33</sup> However, the complex (5), NiCl<sub>2</sub>-piperidine-*p*-MeOAAF, produced no reaction (see Table 2). The Ni(II) complex displays high-spin tendencies and may not reduce to Ni(0) to proceed. Further tests are ongoing. PdCl<sub>2</sub> produced only 18% biphenyl, and a more traditional phosphine-based palladium source, Pd(PPh<sub>3</sub>)<sub>2</sub>Cl<sub>2</sub>, gave 84% of product under these conditions. As a control, the absence of catalyst produced no reaction. Note that the phenylboronic acid pinacol ester was also attempted for this reaction, and under optimized conditions with bromobenzene and catalyst (3a), biphenyl was produced in 84% yield indicating that the boronic acids were not necessary, but under these conditions, were more suitable reagents for Suzuki coupling (see SI).

With the optimal conditions in hand (Table 3, entry 4) using (3a) as precatalyst, the scope of the aryl halides was

**Table 3. Products of Pd-Catalyzed Suzuki–Miyaura Coupling Sequence of Various Aryl Bromides and Phenylboronic Acid<sup>a</sup>**

Entry	R	Yield <sup>b,c</sup> (%)
1	4-MeO	7a, 72 (87)
2	4-Me	7b, 84 (92)
3	4-CHO	7c, 96 (99)
4	4-Cl	7d, 79 (86)
5	4-OH	7e, 71
6	4-CN	7f, 66 (71)
7	2-NH <sub>2</sub>	7g, 79 (87)

<sup>a</sup>Reaction conditions: bromobenzene (1.0 mmol), phenylboronic acid (1.2 mmol), Cs<sub>2</sub>CO<sub>3</sub> (2 mmol), 1,4-dioxane (4 mL), catalyst (1 mol %) 20 h at 90 °C under inert atmosphere. <sup>b</sup>Isolated yield. <sup>c</sup>NMR yield in parentheses.

investigated utilizing phenylboronic acid as a coupling partner. Both electron-donating and -withdrawing groups on the benzene ring were well tolerated to form the corresponding substituted biphenyls (7a–7g), in good to excellent yields (66–96%). Notably, the electronic nature of the aryl bromides appears to have no significant effect on the formation of C–C bond-forming reaction. These findings underscore the versatility and applicability of the reaction methodology across a wide range of electronically distinct substrates.

Next, various arylboronic acids were tested against bromobenzene, and these results are summarized in Table 4. Phenylboronic acids that bear either electron-donating (e.g., 4-Me, 4-OMe) or electron-withdrawing (e.g., 4-CO<sub>2</sub>Me) substituents at the *para*-position readily underwent the coupling reaction with bromobenzene, yielding desired products in moderate yields (refer to Table 4, entries 1, 9, and 12). In contrast, reactions involving *meta* and *ortho*-substituted phenylboronic acids exhibited lower yields for both electron-donating and electron-withdrawing groups when compared to those with *para*-substituted counterparts. This reduction in yield or complete absence of reaction in the case of *ortho*-substituted phenylboronic acids could be attributed to the coordination of the substituent to boron, which slows

**Table 4. Products of Pd-Catalyzed Suzuki–Miyaura Coupling Sequence of Bromobenzene and Various Aryl Boronic Acids<sup>a</sup>**

Entry	R	Yield <sup>b</sup> (%)
1	4-COOCH <sub>3</sub> C <sub>6</sub> H <sub>4</sub>	8a, 67 (72) <sup>b</sup>
2	3-COOCH <sub>3</sub> C <sub>6</sub> H <sub>4</sub>	8b, 57 (64) <sup>c</sup>
3	2-naphthalene	8c, 88 (99) <sup>c</sup>
4	1-naphthalene	8d, 57 (71) <sup>c</sup>
5	3-CH <sub>2</sub> OHC <sub>6</sub> H <sub>4</sub>	8e, 54
6	3-CH <sub>3</sub> SC <sub>6</sub> H <sub>4</sub>	8f, 51
7	3-NO <sub>2</sub> C <sub>6</sub> H <sub>4</sub>	8g, 72
8	2-NO <sub>2</sub> C <sub>6</sub> H <sub>4</sub>	NR
9	4-CH <sub>3</sub> OC <sub>6</sub> H <sub>4</sub>	8h, 58 (61) <sup>b</sup>
10	3-CH <sub>3</sub> OC <sub>6</sub> H <sub>4</sub>	8i, 43 (50) <sup>c</sup>
11	2-CH <sub>3</sub> OC <sub>6</sub> H <sub>4</sub>	8j, 30
12	4-CH <sub>3</sub> C <sub>6</sub> H <sub>4</sub>	8k, 70 (90) <sup>c</sup>
13	2,4,6-(CH <sub>3</sub> ) <sub>3</sub> C <sub>6</sub> H <sub>2</sub>	NR

<sup>a</sup>Reaction conditions: bromobenzene (1.0 mmol), phenyl boronic acid (1.2 mmol), Cs<sub>2</sub>CO<sub>3</sub> (2 mmol), 1,4-dioxane (4 mL), catalyst (1 mol %) 20 h at 90 °C under inert atmosphere. <sup>b</sup>Isolated yield, <sup>c</sup>NMR yield in parentheses, NR = No Reaction.

down the transmetalation step within the catalytic cycle and/or the formation of the catalytic species.<sup>2,34,35</sup> Notably, *ortho*-nitrophenylboronic acid (Table 4, entry 8) showed no reaction, potentially due to hydrogen bonding interactions between the oxygen of the nitro group and the hydroxyl from the boronic acid group, hindering transmetalation. Interestingly, 2,4,6-trimethylphenyl boronic acid did not yield product under the optimized reaction conditions (Table 4, entry 13) indicating that steric bulk impedes the reaction. Furthermore, Naphthalen-2-ylboronic acid provided a significantly higher yield of 88% compared to Naphthalen-1-ylboronic acid (Table 4, entries 3 and 4). This disparity in yield can be attributed to steric effects, with the former benefiting from a more favorable environment. Overall, these findings highlight the interplay of electronic and steric factors in the Pd(II) complex 3a-catalyzed Suzuki–Miyaura cross-coupling reaction and offer insights into the factors that govern the success of this transformation.<sup>34</sup>

Lastly, under optimized conditions with catalyst (3a), the homocoupling reaction of arylboronic acids yielded products (9a–d) and (6) with moderate to good yields with results summarized in Table 5. Specifically, *para*-substituted arylboronic acids with electron-withdrawing and electron-donating groups, such as 4-nitro (4-NO<sub>2</sub>), 4-trifluoromethyl (4-CF<sub>3</sub>) and 4-methoxy (4-MeO), 4-methyl (4-Me), proceeded smoothly, which suggests that electronics do not play an important role in the yield of homocoupled biaryl products under these conditions.

Above, Suzuki–Miyaura catalysis was utilized to analyze AAF ligands and link their unique intricacies of coordination to their utility with palladium(II) chloride. At this point in time the Suzuki–Miyaura reaction is among the most well-studied organometallic transformations, and the general outline of the reaction is understood (i.e., oxidative addition, transmetalation, and reductive elimination).<sup>36–43</sup> In addition to catalysis, Density Functional Theory (DFT) was employed by using B3LYP to provide a possible explanation for the disparity of

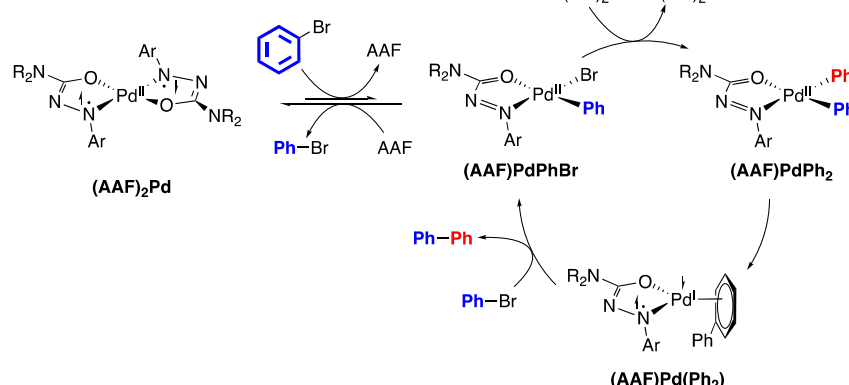
**Table 5. Products of Pd-Catalyzed Suzuki Homocoupling with Various Aryl Boronic Acids<sup>a</sup>**

Entry	R	Yield <sup>b</sup> %
1	4-MeO	9a, 58 (78) <sup>c</sup>
2	4-Me	9b, 30 (35) <sup>c</sup>
3	4-H	6, 70 (79) <sup>c</sup>
4	4-NO <sub>2</sub>	9c, 59 (74) <sup>c</sup>
5	4-CF <sub>3</sub>	9d, 88 (93) <sup>c</sup>

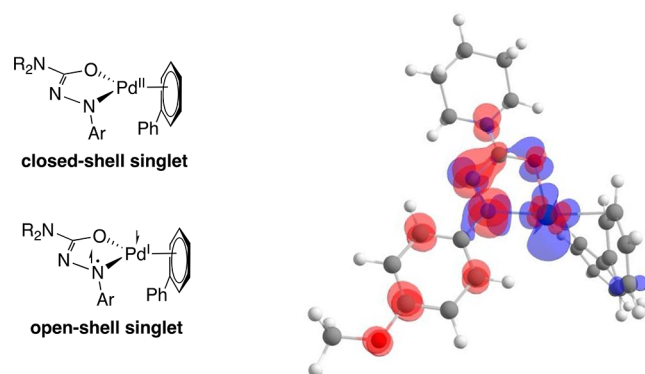
<sup>a</sup>Reaction conditions: phenylboronic acid (1.0 mmol), Cs<sub>2</sub>CO<sub>3</sub> (2.0 mmol), 1,4-dioxane (4 mL), catalyst (1.0 mol %), 20 h at 90 °C under inert atmosphere. <sup>b</sup>Isolated yield. <sup>c</sup>NMR yield in parentheses.

yields and products formed. Specifically, we wished to investigate: (1) the likely resting state of the Pd catalyst during reactivity and (2) provide an explanation for the observed superior activity of the AAF ligand as compared to the ATF ligand. Calculations are largely consistent with the previously established steps for the Suzuki–Miyaura reaction, although the redox-active nature of the AAF and ATF ligands leads to deviations from the standard 2-electron mechanism (Figure 2).

As with all Pd(II)-precatalysts, some means must exist for formal reduction to Pd<sup>0</sup> to enable oxidative addition. Under the reaction conditions outlined above, several formally zerovalent species are possible intermediates during initiation and catalysis. Since the reaction occurs in dioxane (a nonreducing solvent), this likely occurs via 2 equiv of phenylboronic acid to (AAF)PdCl<sub>2</sub> formed in situ from loss of one AAF ligand from the precatalyst. The product of reductive elimination, the biphenyl adduct (AAF)Pd(Ph<sub>2</sub>), is then primed for the displacement of biphenyl by bromobenzene and subsequent oxidative addition. Rather than a genuine Pd<sup>0</sup> species, initial calculations indicate that the biphenyl adduct would be more aptly described as a Pd<sup>II</sup> species and a doubly reduced ligand, although the wave function exhibited an RHF to UHF instability. Further refinement of this structure revealed an open-shell singlet structure 3.13 kcal/mol lower in energy than is best described as a formally Pd<sup>I</sup> species and a singly reduced AAF ligand using the Broken Symmetry formalism (Figure 3).



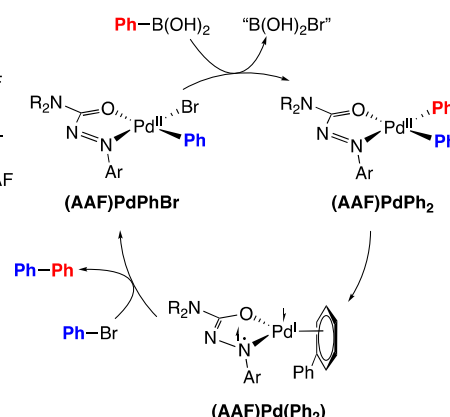
**Figure 2.** Proposed catalytic cycle and intermediates for the AAF-based catalysis, as elucidated by DFT studies.



**Figure 3.** Valence-bond representations of the closed-shell and open-shell singlet structures for (AAF)<sub>2</sub>Pd (left), and a plot of  $\alpha$  (red) and  $\beta$  (blue) spin density for (AAF)Pd(Ph<sub>2</sub>) (right).

The structure of the open-shell singlet is consistent with a Pd<sup>I</sup> species, with most of the  $\beta$ -spin density residing on Pd in an orbital strongly composed of  $d_{x^2-y^2}$ . The biphenyl ligand is best described as bearing a hapticity of  $\eta^2$ , consistent with an overall 17-electron species.<sup>44</sup> During catalysis, biphenyl can also be replaced by an additional equivalent of the starting ligand to yield the bis-ligand complex L<sub>2</sub>Pd (L = ATF or AAF)—this is a likely side-reaction since the precatalysts are of the form L<sub>2</sub>PdCl<sub>2</sub>, and ligands of the ATF type have been shown to dissolve zerovalent metals.<sup>33,45</sup> As for (AAF)Pd(Ph<sub>2</sub>), although closed-shell structures can be found, both the (AAF)<sub>2</sub>Pd and (ATF)<sub>2</sub>Pd complexes exhibit a closed shell to open shell instability in their wave functions and can be further minimized to open-shell singlet structures that can be represented with the Broken Symmetry formalism (Figure 4).

For both (AAF)<sub>2</sub>Pd and (ATF)<sub>2</sub>Pd the energy difference between open- and closed-shell structures is substantial—the open-shell singlet structure is more stable than the closed-shell singlet by 8.09 kcal/mol for (AAF)<sub>2</sub>Pd and 6.97 kcal/mol for (ATF)<sub>2</sub>Pd. Substitution of biphenyl with a second AAF ligand (forming Pd(AAF)<sub>2</sub>) is predicted to be more favorable than oxidative addition (forming (AAF)PdPhBr), but under the low concentration conditions of the catalyst (1 mol % loading), oxidative addition of bromobenzene is still likely competitive in the early stages of the reaction. Nonetheless, the observation of a low yield of biphenyl when using Complex (4) for catalysis may well be due to the stronger tendency of ATF to form the bis-ligand complex relative to AAF.



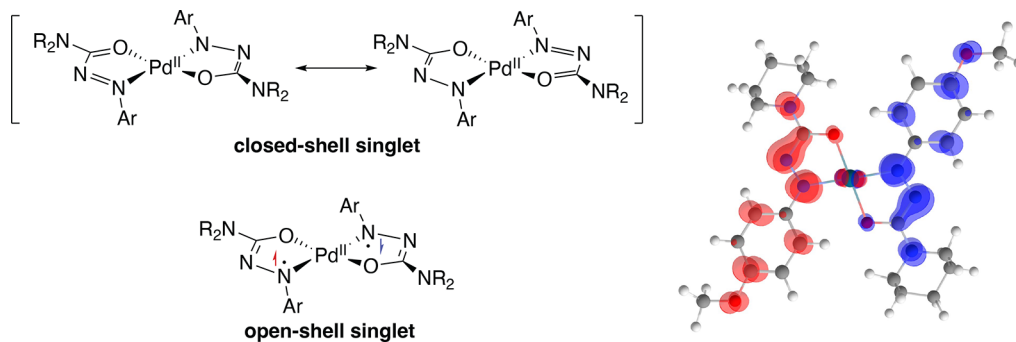


**Figure 4.** Valence-bond representations of the closed-shell and open-shell singlet structures for (AAF)<sub>2</sub>Pd (left), and a plot of  $\alpha$  (red) and  $\beta$  (blue) spin density for (AAF)<sub>2</sub>Pd.

## CONCLUSION

Described was an effective method for Pd-catalyzed Suzuki–Miyaura coupling of aryl bromides with arylboronic acids over a wide range of functional groups, proceeding in good to excellent yields to form the corresponding biphenyls. The  $\text{PdCl}_2(\text{piperidine-}p\text{-MeOAAF})_2$  (**3a**) precatalyst, under optimized conditions, was ideal at 1 mol % loading. Our evaluation demonstrates that the redox activity of the AAF in a Pd(AAF)<sub>2</sub> system allows for an antiferromagnetically coupled open-shell singlet Pd(I) complex. However, nickel(II) complexes were ineffective in promoting the Suzuki–Miyaura reaction. Our aim of this work is to develop and explore robust catalytic systems through ligand design that can contribute to sustainable synthetic practices. Application of this catalyst for the synthesis of small molecule pharmaceuticals and use in other Pd-catalyzed reactions are in progress.

## EXPERIMENTAL SECTION

**General Methods.** <sup>1</sup>H and <sup>13</sup>C NMR experiments were performed on a Bruker AVANCE 300 and 500 MHz. Coupling constants (*J*) are given in Hz. The multiplicities of the signals are described using the following abbreviations: s = singlet, br s = broad singlet, d = doublet, t = triplet, dd = doublet of doublets, dq = doublet of quartets, dsep = doublet of septets; t = triplet of triplets, m = multiplet, app = apparent. Infrared spectra were obtained on a Thermo Scientific Nicolet 380 FT-IR spectrometer as thin films on ZnSe disks, and peaks are reported in  $\text{cm}^{-1}$ . Electrospray ionization mass spectrometry (ESI-MS) was recorded on a Waters Q-TOF Premier mass spectrometer. Elemental Analysis was performed on a Vario microcube Elementar Analyzer. Reaction progress was monitored by thin-layer chromatography on silica gel plates (60-F254), observed under UV light. Column chromatography was performed using silica gel (particle size 40–63  $\mu\text{m}$ ). All reactions were performed under nitrogen atmosphere. 4-Methoxyphenylhydrazine hydrochloride was purchased from AK Scientific, and pyrrolidine was purchased from Alfa-Aesar. Palladium and nickel salts were purchased from Acros, Sigma–Aldrich, or AK Scientific. All aryl halides, arylboronic acids, bases ( $\text{Li}(\text{OH})\text{H}_2\text{O}$ ,  $\text{K}_2\text{CO}_3$ ,  $\text{K}_3\text{PO}_4$ ,  $\text{Cs}_2\text{CO}_3$ , and  $\text{Na}_2\text{CO}_3$ ), DMSO, THF, DMF, toluene, and 1,4-dioxane were purchased from commercial sources. All of the chemicals were used without further purification.

**Procedure for Complex Formation.** *Piperidine p-Methoxy Phenylazoformamide-PdCl<sub>2</sub>* (**3a**) (CCDC: 2340179). 0.4 mmol of synthesized piperidine *p*-methoxy AAF ligand, (**1a**), was dissolved in 5 mL of toluene solvent, and 0.4 mmol of palladium(II) chloride was added to the solution. The mixture was refluxed in a sand bath at 110 °C for 4 h. After cooling to room temperature, the solvent was evaporated. The solid complex was washed with hexane to remove excess ligand and the residue was dissolved with dichloromethane and the solution was decanted and evaporated to obtain orange crystals (0.178 g, 66% yield). <sup>1</sup>H NMR (500 MHz, Chloroform-*d*)  $\delta$  9.07 (d, *J* = 9.2 Hz, 4H, Ar H), 7.03 (d, *J* = 9.2 Hz, 4H, Ar H), 3.93 (s, 6H,  $-\text{OCH}_3$ ), 3.92–3.90 (m, 4H,  $-\text{NCH}_2$ ), 3.37 (t, *J* = 5.2 Hz, 4H,  $-\text{CH}_2\text{N}-$ ), 1.81 (br s, 4H,  $-\text{NCH}_2\text{CH}_2$ ), 1.67–1.65 (m, 8H  $-\text{NCH}_2\text{CH}_2\text{CH}_2\text{CH}_2-$ ).

<sup>13</sup>C NMR (126 MHz,  $\text{CDCl}_3$ )  $\delta$  165.2 (C=O, C1), 159.8 (Ar q, CS), 147.1 (Ar q, C2), 129.4 (Ar CH, C3 and C7), 114.4 (Ar CH, C4 and C6), 56.1 ( $-\text{OCH}_3$ , C13), 46.2 ( $-\text{NCH}_2$ , C12), 44.7 ( $-\text{CH}_2\text{N}-$ , C8), 25.4 (CH<sub>2</sub>, C11), 25.4 (CH<sub>2</sub>, C9), 24.4 (CH<sub>2</sub>, C10). FTIR ( $\text{cm}^{-1}$ ): 2944, 1683 (C=O), 1419 (N=N), 1249 (C–O), 1009, 846. Anal. Calcd for  $\text{C}_{26}\text{H}_{34}\text{Cl}_2\text{N}_6\text{O}_2\text{Pd}$ : C, 46.48; H, 5.10; N, 12.51. Found: C, 46.01; H, 5.478; N, 12.69. Melting point 158 °C

*Pyrrolidine p-Methoxy Phenylazoformamide-PdCl<sub>2</sub>* (**3b**) (CCDC: 2340180). 0.4 mmol of synthesized pyrrolidine *p*-methoxy AAF ligand, (**1b**), was dissolved in 5 mL of toluene solvent, and 0.4 mmol of palladium(II) chloride was added to the solution. The mixture was refluxed in a sand bath at 110 °C for 4 h. After cooling to room temperature, the solvent was evaporated. The solid complex was washed with hexane to remove excess ligand and the residue was dissolved with dichloromethane and the solution was decanted and evaporated to obtain orange crystals (0.166 g, 65% yield). <sup>1</sup>H NMR (500 MHz, Chloroform-*d*)  $\delta$  9.11 (d, *J* = 8.7 Hz, 4H, Ar H), 7.06 (d, *J* = 8.7 Hz, 4H, Ar H), 3.94 (s, 6H,  $-\text{OCH}_3$ ), 3.91–3.86 (m, 4H,  $-\text{NCH}_2$ ), 3.46 (t, *J* = 6.2 Hz, 4H,  $-\text{CH}_2\text{N}-$ ), 1.99–1.94 (m, 8H,  $-\text{NCH}_2\text{CH}_2\text{CH}_2$ ). <sup>13</sup>C NMR (126 MHz,  $\text{CDCl}_3$ )  $\delta$  165.3 (C=O, C1), 159.4 (Ar q, CS), 146.9 (Ar q, C2), 129.5 (Ar CH, C3 and C7), 114.5 (Ar CH, C4 and C6), 56.1 ( $-\text{OCH}_3$ , C12), 47.2 ( $-\text{NCH}_2$ , C11), 46.3 ( $-\text{CH}_2\text{N}-$ , C8), 25.9 (CH<sub>2</sub>, C10), 24.4 (CH<sub>2</sub>, C9). FTIR ( $\text{cm}^{-1}$ ): 2949, 2875, 1691 (C=O), 1494 (N=N), 1263 (C–O), 1001, 839. Anal. Calcd for  $\text{C}_{24}\text{H}_{30}\text{Cl}_2\text{N}_6\text{O}_2\text{Pd}$ : C, 44.77; H, 4.70; N, 13.05. Found: C, 44.91; H, 4.590; N, 13.31. Melting point 151 °C

*Piperidine p-Methoxy Phenylazothioformamide-PdCl<sub>2</sub>* (**4**). 0.4 mmol of synthesized ATF ligand, (**2**), was dissolved in 5 mL of toluene solvent, and 0.4 mmol of palladium(II) chloride was added to the solution. The mixture was refluxed in a sand bath at 110 °C for 4 h. After cooling to room temperature, the solvent was evaporated. The solid complex was washed with hexane to remove excess ligand and the residue was dissolved with dichloromethane and the solution was decanted and evaporated to obtain a dark red solid in (0.132 g, 54% yield). <sup>1</sup>H NMR (500 MHz, Chloroform-*d*)  $\delta$  8.53 (d, *J* = 9.5 Hz, 4H, Ar H), 7.13 (d, *J* = 9.5 Hz, 4H, Ar H), 4.53 (t, *J* = 5.4 Hz, 4H,  $-\text{NCH}_2$ ), 4.42–4.40 (m, 4H,  $-\text{CH}_2\text{N}-$ ), 4.03 (s, 6H,  $-\text{OCH}_3$ ), 2.02 (br s, 4H,  $-\text{NCH}_2\text{CH}_2$ ), 1.92 (p, *J* = 2.6 Hz, 8H,  $-\text{CH}_2\text{CH}_2-$ ). <sup>13</sup>C NMR (126 MHz,  $\text{CDCl}_3$ )  $\delta$  185.1 (C=S, C1), 169.3 (Ar q, CS), 143.8 (Ar q, C2), 124.6 (br Ar CH, C3 and C7), 116.7 (Ar CH, C4 and C6), 56.9 ( $-\text{OCH}_3$ , C8), 55.6 ( $-\text{NCH}_2$ , C9), 52.0 ( $-\text{CH}_2\text{N}$ , C13), 27.6 (CH<sub>2</sub>, C10), 26.4 (CH<sub>2</sub>, C12), 24.1 (CH<sub>2</sub>, C11). FTIR ( $\text{cm}^{-1}$ ): 2929, 1586, 1430 (N=N), 1248 (C–O), 1015 (C=S), 832. Anal. Calcd for  $\text{C}_{26}\text{H}_{34}\text{Cl}_2\text{N}_6\text{O}_2\text{Pd}$ : C, 44.36; H, 4.87; N, 11.94. Found: C, 44.49; H, 4.849; N, 11.82. Melting point 172 °C

*Piperidine p-methoxy phenylazoformamide-NiCl<sub>2</sub>* (**5**) (CCDC: 2340181). 0.4 mmol of synthesized AAF ligand, (**1a**), was dissolved in 5 mL of toluene solvent, and 0.4 mmol of nickel(II)chloride hexahydrate was added to the solution. The mixture was refluxed in

a sand bath at 110 °C for 4 h. After cooling to room temperature, the solvent was evaporated. The solid complex was washed with hexane to remove excess ligand and the residue was dissolved with dichloromethane and the solution was decanted and evaporated to yellowish green crystals (0.175 g, 63% yield). <sup>1</sup>H NMR (500 MHz, Chloroform-*d*)  $\delta$  7.91 (d, *J* = 9.0 Hz, 4H, Ar H), 6.99 (d, *J* = 9.0 Hz, 4H, Ar H), 3.89 (s, 6H,  $-\text{OCH}_3$ ), 3.74–3.70 (m, 4H,  $-\text{NCH}_2$ ), 3.64–3.60 (m, 4H,  $-\text{CH}_2\text{N}-$ ), 1.72–1.68 (m, 8H,  $-\text{CH}_2\text{CH}_2-$ ), 1.63–1.58 (m, 4H,  $-\text{CH}_2-$ ). <sup>13</sup>C NMR (126 MHz, CDCl<sub>3</sub>)  $\delta$  163.8 (C=O, C1), 161.8 (Ar q, C5), 146.7 (Ar q C2), 125.9 (Ar CH, C3 and C7), 114.4 (Ar CH, C4 and C6), 55.8 ( $-\text{OCH}_3$ , C13), 46.1 ( $-\text{NCH}_2$ , C12), 44.7 ( $-\text{CH}_2\text{N}$ , C8), 26.3 (CH<sub>2</sub>, C11), 25.7 (CH<sub>2</sub>, C9), 24.5 (CH<sub>2</sub>, C10). FTIR (cm<sup>-1</sup>): 2958, 1684 (C=O), 1455 (N=N), 1235 (C=O), 1030, 836. Anal. Calcd for C<sub>26</sub>H<sub>34</sub>Cl<sub>2</sub>N<sub>6</sub>O<sub>4</sub>Ni: C, 50.03; H, 5.49; N, 13.34. Found: C, 50.12; H, 5.559; N, 13.31. Melting point 103 °C

**General Procedure for the Suzuki–Miyaura Cross-Coupling Reaction.** A mixture of the appropriate aryl halides (1 mmol), and appropriate phenylboronic acids (1.2 mmol), Pd-complex **3a** (1 mol %), Cs<sub>2</sub>CO<sub>3</sub> (2 mmol), and 1,4-dioxane (4 mL) were stirred at 90 °C for 20 h under inert conditions. The cross-coupled product was then extracted with ethyl acetate (3  $\times$  10 mL). The combined organic extracts were dried over anhydrous MgSO<sub>4</sub>, filtered, and the solvent was evaporated under reduced pressure. The residue was then subjected to separation via flash column chromatography with *n*-hexane or an *n*-hexane/EtOAc mixture as an eluent to give the corresponding pure cross-coupled products.

**General Procedure for Homocoupling.** Arylboronic acids (1.0 mmol), Pd-complex **3a** (1.0 mol %), Cs<sub>2</sub>CO<sub>3</sub> (2.0 mmol), and 1,4-dioxane (4 mL) were stirred at 90 °C for 20 h under inert conditions. The homocoupled product was then extracted with ethyl acetate (3  $\times$  10 mL). The combined organic extracts were dried over anhydrous MgSO<sub>4</sub>, filtered, and the solvent was evaporated under reduced pressure. The residue was then subjected to separation via flash column chromatography with *n*-hexane or an *n*-hexane/EtOAc mixture as an eluent to give the corresponding pure homocoupled products.

**Computational Section.** Calculations were performed using the Gaussian16 software on the Beartooth computational cluster using the B3LYP functional and SDD basis set.<sup>46</sup> All species were optimized in a dioxane solvent using the SMD solvent model, and frequency calculations were performed to determine relative free energies and confirm the absence of imaginary vibrations. Wave functions were checked for stability (and, if necessary, optimized) using the keyword stable = opt. Spin density plots were generated with the Chemcraft visualization software.<sup>47</sup>

## ASSOCIATED CONTENT

### Data Availability Statement

The data underlying this study are available in the published article and its [Supporting Information](#).

### Supporting Information

The Supporting Information is available free of charge at <https://pubs.acs.org/doi/10.1021/acs.joc.4c01062>.

#### Atomic coordinates (XYZ)

Experimental procedures for **1a**, **1b**, **2** and the characterization data; characterization data for all Suzuki cross- and homo- coupled products; <sup>1</sup>H and <sup>13</sup>C NMR spectra; Mass spectra of ligands; X-ray diffraction data for compounds **1a-b**, **2**, **3a-b** and **5**; computational results; 2D NMR. ([PDF](#))

### Accession Codes

Deposition Numbers [2330627](#) and [2340177–2340181](#) contain the supplementary crystallographic data for this paper. These data can be obtained free of charge via the joint Cambridge Crystallographic Data Centre (CCDC) and Fachinformationszentrum Karlsruhe [Access Structures service](#).

## AUTHOR INFORMATION

### Corresponding Authors

Kristopher V. Waynant – Department of Chemistry, University of Idaho, Moscow, Idaho 83844, United States;  [orcid.org/0000-0002-4096-5726](#); Email: [kwaynant@uidaho.edu](mailto:kwaynant@uidaho.edu)

Elliott B. Hulley – Department of Chemistry, University of Wyoming, Laramie, Wyoming 82071, United States;  [orcid.org/0000-0002-2630-3689](#); Email: [ehulley@uwyo.edu](mailto:ehulley@uwyo.edu)

### Author

Laxmi Tiwari – Department of Chemistry, University of Idaho, Moscow, Idaho 83844, United States;  [orcid.org/0009-0004-6103-4471](#)

Complete contact information is available at: <https://pubs.acs.org/10.1021/acs.joc.4c01062>

### Notes

The authors declare no competing financial interest.

## ACKNOWLEDGMENTS

The project was supported by an Institutional Development Award (IDeA) from the National Institute of General Medical Sciences of the National Institutes of Health under Grant #P20GM103408 (Idaho) and 2P20GM103432 (Wyoming). X-ray crystallographic data were collected at the University of Montana X-ray diffraction core facility supported by the Center for Biomolecular Structure and Dynamics CoBRE (National Institutes of Health, CoBRE NIGMS P30GM-103546). Single crystal X-ray diffraction data were collected using a Bruker D8 Venture, principally supported by NSF MRI CHE-1337908.

## REFERENCES

- Wu, X.; Anbarasan, P.; Neumann, H.; Beller, M. From Noble Metal to Nobel Prize: Palladium-Catalyzed Coupling Reactions as Key Methods in Organic Synthesis. *Angew. Chem., Int. Ed.* **2010**, *49* (48), 9047–9050.
- Miyaura, N.; Suzuki, A. Stereoselective Synthesis of Arylated (E)-Alkenes by the Reaction of Alk-1-Enylboranes with Aryl Halides in the Presence of Palladium Catalyst. *J. Chem. Soc. Chem. Commun.* **1979**, No. 19, 866.
- Nicolaou, K. C.; Bulger, P. G.; Sarlah, D. Palladium-Catalyzed Cross-Coupling Reactions in Total Synthesis. *Angew. Chem., Int. Ed.* **2005**, *44* (29), 4442–4489.
- Palladium-Catalyzed Coupling Reactions: Practical Aspects and Future Developments; Molnár, A., Ed.; Wiley-VCH: Weinheim, Germany, 2013.
- Littke, A. F.; Dai, C.; Fu, G. C. Versatile Catalysts for the Suzuki Cross-Coupling of Arylboronic Acids with Aryl and Vinyl Halides and Triflates under Mild Conditions. *J. Am. Chem. Soc.* **2000**, *122* (17), 4020–4028.
- Zhang, C.; Huang, J.; Trudell, M. L.; Nolan, S. P. Palladium-Imidazol-2-Ylidene Complexes as Catalysts for Facile and Efficient Suzuki Cross-Coupling Reactions of Aryl Chlorides with Arylboronic Acids. *J. Org. Chem.* **1999**, *64* (11), 3804–3805.
- Shaikh, T. M.; Weng, C.-M.; Hong, F.-E. Secondary Phosphine Oxides: Versatile Ligands in Transition Metal-Catalyzed Cross-Coupling Reactions. *Coord. Chem. Rev.* **2012**, *256* (9–10), 771–803.
- De Meijere, A.; Meyer, F. E. Fine Feathers Make Fine Birds: The Heck Reaction in Modern Garb. *Angew. Chem., Int. Ed. Engl.* **1995**, *33* (23–24), 2379–2411.

(9) Zhou, J.; Fu, G. C. Suzuki Cross-Couplings of Unactivated Secondary Alkyl Bromides and Iodides. *J. Am. Chem. Soc.* **2004**, *126* (5), 1340–1341.

(10) Tao, B.; Boykin, D. W. Simple Amine/Pd(OAc)<sub>2</sub>-Catalyzed Suzuki Coupling Reactions of Aryl Bromides under Mild Aerobic Conditions. *J. Org. Chem.* **2004**, *69* (13), 4330–4335.

(11) Mino, T.; Shirae, Y.; Sakamoto, M.; Fujita, T. Phosphine-Free Hydrazine-Pd Complex as the Catalyst Precursor for a Suzuki-Miyaura Reaction under Mild Aerobic Conditions. *J. Org. Chem.* **2005**, *70* (6), 2191–2194.

(12) Liu, T.; Zhao, X.; Shen, Q.; Lu, L. General and Highly Efficient Fluorinated-N-Heterocyclic Carbene-Based Catalysts for the Palladium-Catalyzed Suzuki-Miyaura Reaction. *Tetrahedron* **2012**, *68* (32), 6535–6547.

(13) Susanto, W.; Chu, C.-Y.; Ang, W. J.; Chou, T.-C.; Lo, L.-C.; Lam, Y. Development of a Fluorous, Oxime-Based Palladacycle for Microwave-Promoted Carbon–Carbon Coupling Reactions in Aqueous Media. *Green Chem.* **2012**, *14* (1), 77–80.

(14) Yadav, J. S.; Gayathri, K. U.; Ather, H.; Rehman, H. U.; Prasad, A. R. Utility of Semicarbazones as Ligands in Newly Made Palladium Complex for Facile Suzuki Homocoupling Reaction of Alkyl and Aryl Boronic Acids. *J. Mol. Catal. Chem.* **2007**, *271* (1–2), 25–27.

(15) Tiwari, L.; Waynant, K. V. The Synthesis and Structural Properties of a chloridobis{N-[4-Methoxyphenyl]Imino}Pyrrolidine-1-Carboxamide}zinc(II) Trichloridozincate Coordination Complex. *Acta Crystallographica Section E* **2024**, *80*, 14–17.

(16) Pradhan, R.; Groner, V. M.; Gutman, K. L.; Larson, G. E.; Kan, Y.; Zhang, Q.; Heiden, Z. M.; Roll, M. F.; Moberly, J. G.; Waynant, K. V. Evaluating Coordinative Binding Mechanisms through Experimental and Computational Studies of Methoxy-Substituted Arylazothioformamide Copper(I) Complexes. *Eur. J. Inorg. Chem.* **2022**, *2022* (33), No. e202200421.

(17) Pradhan, R.; Tiwari, L.; Groner, V. M.; Leach, C.; Lusk, K.; Harrison, N. S.; Cornell, K. A.; Waynant, K. V. Evaluation of Azothioformamides and Their Copper(I) and Silver(I) Complexes for Biological Activity. *J. Inorg. Biochem.* **2023**, *246*, 112294.

(18) Johnson, N. A.; Wolfe, S. R.; Kabir, H.; Andrade, G. A.; Yap, G. P. A.; Heiden, Z. M.; Moberly, J. G.; Roll, M. F.; Waynant, K. V. Deconvoluting the Innocent vs. Non-Innocent Behavior of N,N-Diethylphenylazothioformamide Ligands with Copper Sources. *Eur. J. Inorg. Chem.* **2017**, *2017* (47), 5576–5581.

(19) Meconi, G. M.; Vummala, S. V. C.; Luque-Urrutia, J. A.; Belanzoni, P.; Nolan, S. P.; Jacobsen, H.; Cavallo, L.; Solà, M.; Poater, A. Mechanism of the Suzuki-Miyaura Cross-Coupling Reaction Mediated by [Pd(NHC)(Allyl)Cl] Precatalysts. *Organometallics* **2017**, *36* (11), 2088–2095.

(20) Shen, D.; Xu, Y.; Shi, S.-L. A Bulky Chiral N-Heterocyclic Carbene Palladium Catalyst Enables Highly Enantioselective Suzuki-Miyaura Cross-Coupling Reactions for the Synthesis of Biaryl Atropisomers. *J. Am. Chem. Soc.* **2019**, *141* (37), 14938–14945.

(21) Szilvási, T.; Veszprémi, T. Internal Catalytic Effect of Bulky NHC Ligands in Suzuki-Miyaura Cross-Coupling Reaction. *ACS Catal.* **2013**, *3* (9), 1984–1991.

(22) Altenhoff, G.; Goddard, R.; Lehmann, C. W.; Glorius, F. An N-Heterocyclic Carbene Ligand with Flexible Steric Bulk Allows Suzuki Cross-Coupling of Sterically Hindered Aryl Chlorides at Room Temperature. *Angew. Chem., Int. Ed.* **2003**, *42* (31), 3690–3693.

(23) Dai, S.; Sui, X.; Chen, C. Highly Robust Palladium(II)  $\alpha$ -Diimine Catalysts for Slow-Chain-Walking Polymerization of Ethylene and Copolymerization with Methyl Acrylate. *Angew. Chem., Int. Ed.* **2015**, *54* (34), 9948–9953.

(24) Dai, S.; Zhou, S.; Zhang, W.; Chen, C. Systematic Investigations of Ligand Steric Effects on  $\alpha$ -Diimine Palladium Catalyzed Olefin Polymerization and Copolymerization. *Macromolecules* **2016**, *49* (23), 8855–8862.

(25) Barder, T. E.; Walker, S. D.; Martinelli, J. R.; Buchwald, S. L. Catalysts for Suzuki-Miyaura Coupling Processes: Scope and Studies of the Effect of Ligand Structure. *J. Am. Chem. Soc.* **2005**, *127* (13), 4685–4696.

(26) Pradhan, R.; Gutman, K. L.; Mas Ud, A.; Hulley, E. B.; Waynant, K. V. Catalytic Carboxylation of Terminal Alkynes with Copper(I) Azothioformamide Complexes. *Organometallics* **2023**, *42* (5), 362–371.

(27) Pradhan, R.; Groner, V. M.; Gutman, K. L.; Heiden, Z. M.; Roll, M. F.; Moberly, J. G.; Waynant, K. V. Substitution Effects on the Binding Interactions of Redox-Active Arylazothioformamide Ligands and Copper(I) Salts. *Supramol. Chem.* **2020**, *32* (8), 466–478.

(28) Lyaskovsky, V.; de Bruin, B. Redox Non-Innocent Ligands: Versatile New Tools to Control Catalytic Reactions. *ACS Catal.* **2012**, *2* (2), 270–279.

(29) Kostas, I. D.; Steele, B. R. Thiosemicarbazone Complexes of Transition Metals as Catalysts for Cross-Coupling Reactions. *Catalysts* **2020**, *10* (10), 1107.

(30) Yan, H.; Chellan, P.; Li, T.; Mao, J.; Chibale, K.; Smith, G. S. Cyclometallated Pd(II) Thiosemicarbazone Complexes: New Catalyst Precursors for Suzuki-Coupling Reactions. *Tetrahedron Lett.* **2013**, *54* (2), 154–157.

(31) Li, H.; Zhong, Y.-L.; Chen, C.; Ferraro, A. E.; Wang, D. A Concise and Atom-Economical Suzuki-Miyaura Coupling Reaction Using Unactivated Trialkyl- and Triarylborationes with Aryl Halides. *Org. Lett.* **2015**, *17* (14), 3616–3619.

(32) Tiwari, L.; Leach, C.; Williams, A.; Lighter, B.; Heiden, Z. M.; Roll, M. F.; Moberly, J. G.; Cornell, K. A.; Waynant, K. V. Binding Mechanisms and Therapeutic Activity of Heterocyclic Substituted Arylazothioformamide Ligands and Their Cu(I) Coordination Complexes. *ACS Omega* **2024**, *9*, 37141.

(33) Nielsen, K. T.; Bechgaard, K.; Krebs, F. C. Removal of Palladium Nanoparticles from Polymer Materials. *Macromolecules* **2005**, *38* (3), 658–659.

(34) Li, X.; Zou, G. Acylative Suzuki Coupling of Amides: Acyl-Nitrogen Activation via Synergy of Independently Modifiable Activating Groups. *Chem. Commun.* **2015**, *51* (24), 5089–5092.

(35) Tamang, S. R.; Achazi, A. J.; Rust, H. S.; Dhungana, P.; Miró, P.; Hoefelmeyer, J. D. Suzuki Coupling Catalyzed by Chloro{2-[Mesityl(Quinolin-8-Yl- $\kappa$ N)Boryl]-3,5-Dimethylphenyl}methyl- $\kappa$ C-Palladium(II). *Tetrahedron* **2019**, *75* (16), 2365–2370.

(36) Ortúñoz, M. A.; Lledós, A.; Maseras, F.; Ujaque, G. The Transmetalation Process in Suzuki-Miyaura Reactions: Calculations Indicate Lower Barrier via Boronate Intermediate. *ChemCatChem.* **2014**, *6* (11), 3132–3138.

(37) García-Melchor, M.; Braga, A. A. C.; Lledós, A.; Ujaque, G.; Maseras, F. Computational Perspective on Pd-Catalyzed C–C Cross-Coupling Reaction Mechanisms. *Acc. Chem. Res.* **2013**, *46* (11), 2626–2634.

(38) Zhao, X.; Zhang, D.; Wang, X. Unraveling the Mechanism of Palladium-Catalyzed Base-Free Cross-Coupling of Vinyl Carboxylates: Dual Role of Arylboronic Acids as a Reducing Agent and a Coupling Partner. *ACS Catal.* **2022**, *12* (3), 1809–1817.

(39) Braga, A. A. C.; Morgan, N. H.; Ujaque, G.; Lledós, A.; Maseras, F. Computational Study of the Transmetalation Process in the Suzuki-Miyaura Cross-Coupling of Aryls. *Theory Mech. Stud.* **2006**, *691* (21), 4459–4466.

(40) Sperger, T.; Sanhueza, I. A.; Kalvet, I.; Schoenebeck, F. Computational Studies of Synthetically Relevant Homogeneous Organometallic Catalysis Involving Ni, Pd, Ir, and Rh: An Overview of Commonly Employed DFT Methods and Mechanistic Insights. *Chem. Rev.* **2015**, *115* (17), 9532–9586.

(41) Braga, A. A. C.; Ujaque, G.; Maseras, F. A DFT Study of the Full Catalytic Cycle of the Suzuki-Miyaura Cross-Coupling on a Model System. *Organometallics* **2006**, *25* (15), 3647–3658.

(42) Kozuch, S.; Martin, J. M. L. What Makes for a Bad Catalytic Cycle? A Theoretical Study on the Suzuki-Miyaura Reaction within the Energetic Span Model. *ACS Catal.* **2011**, *1* (4), 246–253.

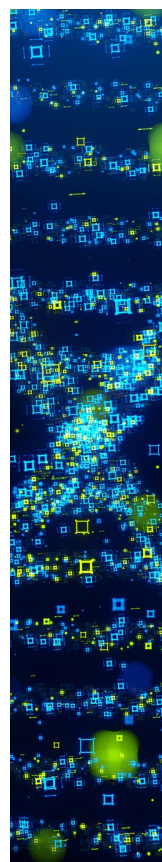
(43) Lakmini, H.; Ciofini, I.; Jutand, A.; Amatore, C.; Adamo, C. Pd-Catalyzed Homocoupling Reaction of Arylboronic Acid: Insights from Density Functional Theory. *J. Phys. Chem. A* **2008**, *112* (50), 12896–12903.

(44) Bruckhoff, T.; Ballmann, J.; Gade, L. H. Radicalizing CO by Mononuclear Palladium(I). *Angew. Chem., Int. Ed.* **2024**, *63* (19), No. e202320064.

(45) Nielsen, K.; Bechgaard, K.; Krebs, F. Effective Removal and Quantitative Analysis of Pd, Cu, Ni, and Pt Catalysts from Small-Molecule Products. *Synth.-Stuttg.* **2006**, *2006* (10), 1639–1644.

(46) Frisch, M. J.; Trucks, G. W.; Schlegel, H. B.; Scuseria, G. E.; Robb, M. A.; Cheeseman, J. R.; Scalmani, G.; Barone, V.; Petersson, G. A.; Nakatsuji, H.; Li, X.; Caricato, M.; Marenich, A. V.; Bloino, J.; Janesko, B. G.; Gomperts, R.; Mennucci, B.; Hratchian, H. P.; Ortiz, J. V.; Izmaylov, A. F.; Sonnenberg, J. L.; Williams-Young, D.; Ding, F.; Lipparini, F.; Egidi, F.; Goings, J.; Peng, B.; Petrone, A.; Henderson, T.; Ranasinghe, D.; Zakrzewski, V. G.; Gao, J.; Rega, N.; Zheng, G.; Liang, W.; Hada, M.; Ehara, M.; Toyota, K.; Fukuda, R.; Hasegawa, J.; Ishida, M.; Nakajima, T.; Honda, Y.; Kitao, O.; Nakai, H.; Vreven, T.; Throssell, K.; Montgomery, J. A., Jr.; Peralta, J. E.; Ogliaro, F.; Bearpark, M. J.; Heyd, J. J.; Brothers, E. N.; Kudin, K. N.; Staroverov, V. N.; Keith, T. A.; Kobayashi, R.; Normand, J.; Raghavachari, K.; Rendell, A. P.; Burant, J. C.; Iyengar, S. S.; Tomasi, J.; Cossi, M.; Millam, J. M.; Klene, M.; Adamo, C.; Cammi, R.; Ochterski, J. W.; Martin, R. L.; Morokuma, K.; Farkas, O.; Foresman, J. B.; Fox, D. J. *Gaussian 16*, Revision C.01; Gaussian, Inc.: Wallingford, CT, 2016.

(47) Chemcraft - Graphical Software for Visualization of Quantum Chemistry Computations. Version 1.8, Build 682. [Https://Www.Chemcraftprog.Com](https://Www.Chemcraftprog.Com).



CAS BIOFINDER DISCOVERY PLATFORM™

**STOP DIGGING  
THROUGH DATA  
— START MAKING  
DISCOVERIES**

CAS BioFinder helps you find the right biological insights in seconds

**Start your search**

